

## Original Research Article

# Enhancement of solubility and dissolution rate of atorvastatin calcium by co-crystallization

Yudi Wicaksono<sup>1,2\*</sup>, Budipratiwi Wisudyaningsih<sup>1</sup> and Tri A Siswoyo<sup>2</sup>

<sup>1</sup>Faculty of Pharmacy, <sup>2</sup>Center for Development of Advanced Science and Technology, University of Jember, Jember, Indonesia

\*For correspondence: **Email:** [yudi.farmasi@unej.ac.id](mailto:yudi.farmasi@unej.ac.id); **Tel:** +62-85859421020

Sent for review: 16 November 2016

Revised accepted: 17 June 2017

### Abstract

**Purpose:** To investigate the formation of atorvastatin calcium (AC) co-crystal to improve its solubility and dissolution rate.

**Method:** Co-crystallization of AC in equimolar ratio with isonicotinamide (INA) was carried out by slow solvent evaporation method using methanol. The solid obtained was characterized by powder x-ray diffraction (PXRD), differential scanning calorimetry (DSC), Fourier transform infrared spectroscopy (FTIR), scanning electron microscopy (SEM), and then further evaluated for solubility and dissolution.

**Results:** The PXRD pattern of ACINA showed new crystalline peaks at  $2\theta$  values of 8.2 and 18.3°, indicating the presence of a new crystalline phase of ACINA co-crystal. The DSC thermogram of ACINA displayed a melting point at 201.7 °C which is higher than the melting points of AC (159.4 °C) and INA (158.0 °C). The FTIR spectra of AC in ACINA shifted the absorption peak from 3363 to 3280  $\text{cm}^{-1}$  and to 1216 to 1222  $\text{cm}^{-1}$ . The absorption peak shift is presumably due to N-H and C-N groups of AC form the hydrogen bonding interaction with groups in INA molecule. The solubility of ACINA co-crystal in distilled water was 270.7 mg/L which is significantly higher ( $p < 0.05$ ) than that of pure AC (140.9 mg/L). The dissolution rate of ACINA co-crystal was 2 - 3 times faster than that of pure AC.

**Conclusion:** AC and INA in equimolar ratio forms a co-crystal by slow solvent evaporation. ACINA co-crystal significantly increases in solubility with a dissolution rate 2 - 3 times faster than that of pure AC. The enhancement of aqueous solubility and dissolution rate of AC with co-crystallization may be a potential way to solving the bioavailability problem of AC.

**Keywords:** Atorvastatin calcium, Co-crystal, Isonicotinamide, Solubility, Dissolution rate

Tropical Journal of Pharmaceutical Research is indexed by Science Citation Index (SciSearch), Scopus, International Pharmaceutical Abstract, Chemical Abstracts, Embase, Index Copernicus, EBSCO, African Index Medicus, JournalSeek, Journal Citation Reports/Science Edition, Directory of Open Access Journals (DOAJ), African Journal Online, Bioline International, Open-J-Gate and Pharmacy Abstracts

## INTRODUCTION

Atorvastatin calcium (AC),  $[(R-(R^*,R^*))\text{-}2\text{-(4-fluorophenyl)-}\beta\text{-, delta-dihydroxy-5-(1-methylethyl)-3-phenyl-4-[(phenylamino)carbonyl]-1H-pyrrole-1-heptanoic acid)]$ , which is calcium salt (2:1) trihydrate ( $[\text{C}_{33}\text{H}_{34}\text{FN}_2\text{O}_5]_2\text{Ca}\cdot 3\text{H}_2\text{O}$ ), is considered one of the most effective synthetic lipid lowering agents [1,2]. The drug is administered orally to reduce total cholesterol, low density lipoprotein and triglycerides [3]. AC

has very good intestinal permeability but it has poor aqueous solubility [4]. This is caused oral by the bioavailability of AC of only about 12 - 14 % [1,5]. Thus, enhancement of aqueous solubility of AC may be a potential way to solving the bioavailability problem of AC [3].

Co-crystallization is one of the techniques generally implemented by researchers to fix the physicochemical properties of an active pharmaceutical ingredient (API) [6-8]. Co-crystal

is defined as a non-single component system consisting of various components that are completely solid under ambient conditions and attached with non-covalent bonds such as hydrogen bonds, aromatic-aromatic interactions and van der Waals bonds [6,9,10].

A pharmaceutical co-crystal normally consists of two types: API and an API with appropriate co-former. The most frequently used co-formers to form pharmaceutical co-crystal are carboxylic acids and amides [11]. Co-crystallization of API is the most frequently selected technique to optimize physicochemical properties while retaining its molecular structure. The physicochemical properties apparently proven to be fixed through co-crystallization are solubility, dissolution rate, moisture uptake, stability, and bioavailability [12].

The most common methods for production of co-crystals are solution crystallization, mechanical grinding and melt crystallization. However, there are other techniques such as fast evaporation, super-critical fluids, addition of anti-solvent, sonic-slurring, melt-extrusion, wet compression, dry compression [9,13]. Co-crystallization by evaporation of stoichiometric solutions is the general technique to prepare of co-crystal [11].

The main objective of the present work was to investigate the formation of AC co-crystal in order to enhance the solubility and dissolution rate of AC.

## EXPERIMENTAL

### Materials

AC was a gift from PT Dexa Medica (Indonesia). INA and methanol were obtained from Sigma-Aldrich (France) and Smart Lab (Indonesia), respectively.

### Co-crystallization of ACINA

Co-crystallization was achieved by the slow solvent evaporation method. AC and INA in equimolar ratio (1:1) were placed into the glass beaker then added methanol and stirred with a magnetic stirrer until dissolved. The glass beaker was covered with aluminum foil and given the small holes. The solution in glass beaker was allowed at room temperature for slowly evaporation of the solvent. The solid of ACINA was obtained then crushed and characterized by PXRD, DSC, FTIR, SEM and further examined by solubility and dissolution test.

## Characterization of co-crystal

### Powder x-ray diffraction

Philip Xpert diffractometer with Cu K $\alpha$  radiation (1.54060 Å) is used for diffractogram X-ray check of sample. The divergence slit and anti-scattering slit condition was set at 0.25° with diffraction experiment on the 10-mm sample size. The measurement was carried out 5-50° in 2 $\theta$  with a step size of 0.017° and a step time of 10 s/step.

### Differential scanning calorimetry

Rigaku Thermo Plus EVO II was used in the analysis of DSC samples. Sealed aluminium pans were used as the container of approximately 2 mg sample and the measurement was applied at 50 -250 °C with 10 °C/min heating rate. The dry nitrogen atmosphere was conducted in the experiments.

### Fourier transform-infrared spectroscopy

ALPHA Bruker spectrometer was applied for the measurement of FTIR spectra of samples. The FTIR spectra of samples were taken using a spectra resolution of 4 cm<sup>-1</sup> in the wavenumber range of 4000-600 cm<sup>-1</sup>.

### Scanning electron microscopy

Prior to the experiment, samples were coated with platinum using ion sputter coater Hitachi E-1045 for 10 seconds. The SEM of samples was then examined using TM 3000 (Hitachi Tabletop Microscope) with observation condition modes on accelerating voltage 15 kV and magnification 500 times.

### Solubility studies

The solubility of AC co-crystal and pure AC in distilled water were determined by shake-flask method. An excess of each sample was placed in Erlenmeyer flask and water added. The resulting suspension was moved into orbital incubator (Stuart S1600) at 37 ± 0.5 °C and continuously shaken at 150 rpm for 12 h. Sample was then filtered using membrane filter (cellulose nitrate 0.45 µm pore size) and the filtrate absorption was measured by double beam spectrophotometer (Hitachi U-2900). The solubility experiments were repeatedly carried out three times.

### Dissolution test

The sample powder was sieved with a size 80 mesh sieve so that the sample powder was

produced with a similar particle size distribution. Dissolution tests were conducted using USP apparatus with a stirring speed of 150 rpm and a temperature of  $37 \pm 0.5$  °C. The test was carried out with a distilled water dissolution medium of 900 mL and a sample amount of 25 mg equivalent of AC. Sampling was carried out at 15, 30, 45, 60, 90 and 120 min and replacement of new media with the same amount after each sampling. The sample was filtered with a cellulose nitrate membrane filter of 0.45  $\mu\text{m}$  and then filtrate concentration was measured using UV-Vis spectrophotometer (Hitachi U-2900). Dissolution test was repeated three times.

### Statistical analysis

The statistical analysis was conducted using one way analysis of variance (ANOVA) of SPSS version 16.0 for windows. The differences of average values were considered to be significant at  $p < 0.05$ .

## RESULTS

### Powder x-ray diffractograms

PXRD was used to detect formation of co-crystal. The PXRD patterns of AC, INA and ACINA are displayed in Figure 1. PXRD pattern of AC presenting specific diffraction peaks at  $2\theta$  values of 10.0, 11.6, 19.3 and 21.4, while INA had specific diffraction peaks at  $2\theta$  values of 17.6, 20.7, 23.3 and 25.7°. ACINA had displayed crystalline peaks of PXRD pattern at  $2\theta$  values of 8.2 and 18.3°.

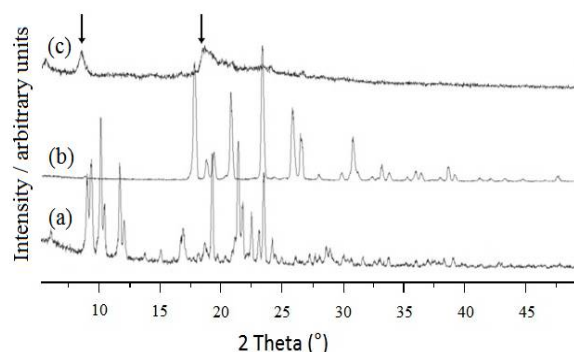
### DSC thermograms

Figure 2 shows DSC curves of AC, INA and ACINA. AC has two endothermic peaks that is one peak at 108.5°C and the other is at 159.4°C, whereas INA has one sharp endothermic peak at 158.0°C. DSC curve of ACINA showed different endothermic peak with AC and INA, which was observed at 201.7°C.

### Fourier transform infrared spectra

The FTIR spectra of AC, INA, and ACINA are illustrated in Figure 3. AC has characteristic spectra with a sharp absorption peak at 3373  $\text{cm}^{-1}$  indicating O-H stretching (free), aromatic N-H stretching at 3363  $\text{cm}^{-1}$ , C=O stretching at 1649  $\text{cm}^{-1}$  and C-N stretching at 1216  $\text{cm}^{-1}$ . FTIR spectra of INA showed N-H stretching at 3368 and 3184  $\text{cm}^{-1}$ , C=O stretching of carboxylic acid at 1658  $\text{cm}^{-1}$ ,  $\text{NH}_2$  stretching at 1623  $\text{cm}^{-1}$ , C-N stretching at 1394  $\text{cm}^{-1}$  and O-C-N stretching at 630  $\text{cm}^{-1}$ . The FTIR spectra of ACINA has

characteristic absorption peaks at 3280, 1648, 1555 and 1221  $\text{cm}^{-1}$ .



**Figure 1:** PXRD patterns of (a) AC, (b) INA and (c) ACINA

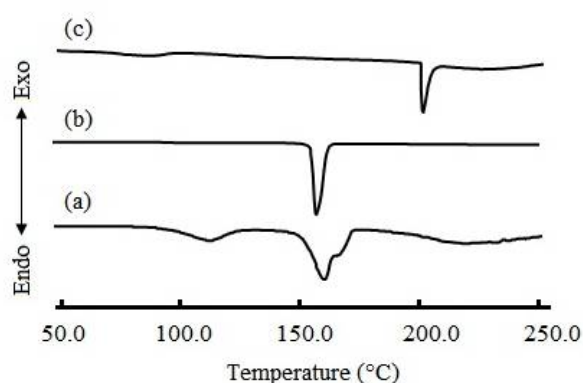


**Figure 2:** DSC curves of (a) AC, (b) INA and (c) ACINA

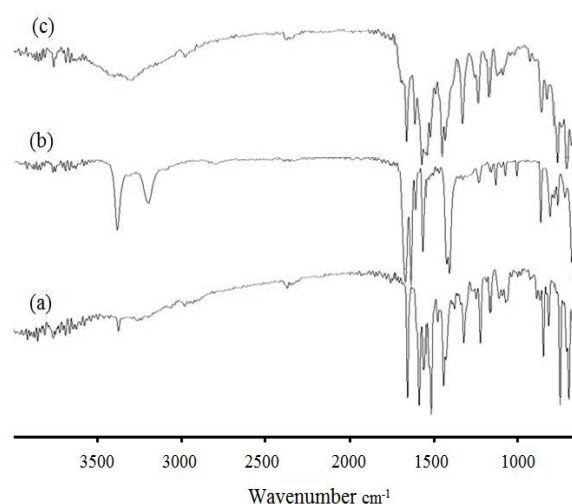


**Figure 3:** FTIR spectra of (a) AC, (b) INA and (c) ACINA

### Morphology

Figure 4 shows SEM images of AC, INA and ACINA. The shape of AC particle has acicular with size of length approximately about 30-100

$\mu\text{m}$ , while INA has angular-shaped particles with a size of approximately  $100 \mu\text{m}$ . The shape of particle of ACINA has spherical irregular with rough surfaces.

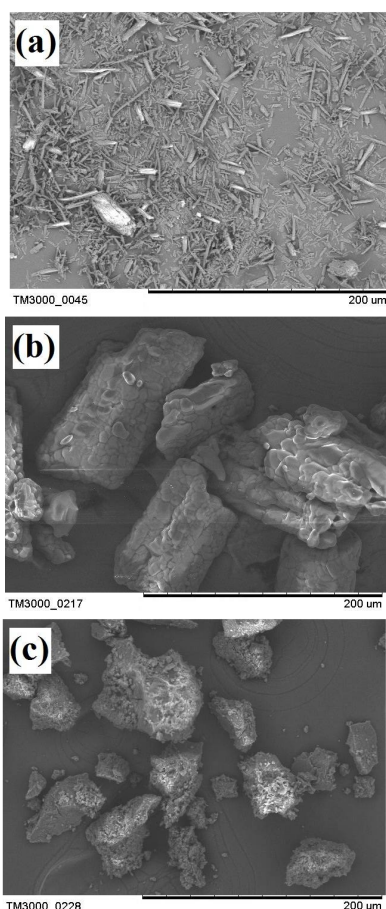


**Figure 4:** SEM images of (a) AC, (b) INA and (c) ACINA

### Solubility

The solubility of ACINA and pure AC were determined in distilled water. The solubility of pure AC and ACINA in distilled water are  $140.9 \text{ mg/L}$  and  $270.7 \text{ mg/L}$ , respectively. Result founded that the solubility of AC from ACINA was significantly higher than pure AC ( $p < 0.05$ ).

### Dissolution rate

The dissolution profiles of ACINA and pure AC are presented in Figure 5. ACINA reached AC dissolution  $74 \%$  within  $15 \text{ min}$ . However, only  $24 \%$  of pure AC was dissolved during the same period. After  $120 \text{ min}$ , about  $92 \%$  of AC was dissolved from ACINA, while only  $50 \%$  of pure AC was dissolved.

## DISCUSSION

Each crystalline substance has unique and

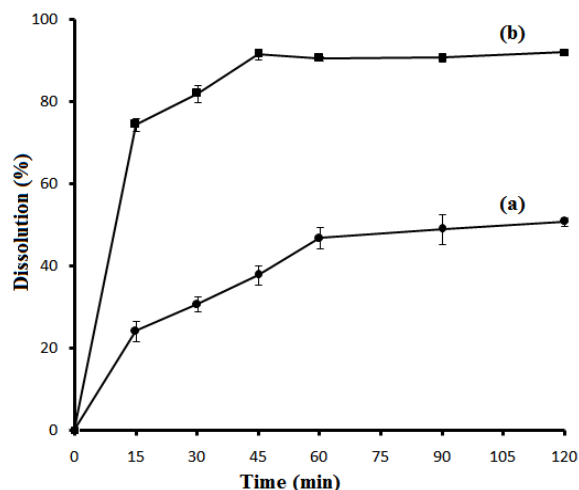


**Figure 5:** Dissolution profiles of (a) AC and (b) ACINA

specific PXRD pattern. It is the fingerprint of the crystalline materials indicating the reflections of specific atomic planes [14,15]. PXRD pattern of ACINA was different from those of the individual pattern of AC and INA. These new PXRD patterns of ACINA indicate the presence of a new crystalline phase of ACINA [16,17].

In the research of physicochemical properties of drugs, thermal properties play a pivotal role as it is an indicator of other drug properties. DSC measurement is one method of thermal properties check used to detect the formation of co-crystal [13]. In the DSC thermogram, the formation of co-crystal is characterized by a single endothermic peak different from other initial components. The new endothermic peak indicates the melting point of the co-crystal phase [18].

DSC curves of AC showed abroad peak at  $108.5 \text{ }^\circ\text{C}$  which depict water loss, followed by a second endothermic peak due to water loss and melting at  $159.4 \text{ }^\circ\text{C}$  [1]. The DSC curve of INA has one endothermic peak at  $158.0 \text{ }^\circ\text{C}$  due to the melting point of INA. The ACINA has a sharp endothermic peak at  $201.7 \text{ }^\circ\text{C}$ , indicating the fusion of ACINA. Based on the DSC curve of ACINA it turns out that AC and INA have a lower melting point than ACINA's co-crystal melting point.

FTIR spectroscopy is one of the commonly used methods to identify co-crystal conformation. With the analysis of FTIR spectra the conformation structure among the functional groups of the constituent components of the co-crystal can be estimated. The interaction between functional groups in the co-crystal will result in a shift in the peaks of FTIR spectra absorption compared to

its individual component [11]. The interaction of functional groups on the co-crystal through hydrogen bonds of the amide-acid group will shift the frequency of absorption of both OH and NH groups towards the individual component absorption frequency. The hydrogen bond usually causes a red shift in the co-crystal as the hydrogen bond apparently stronger in the co-crystal than each of the constituents [19].

The shifting of peaks was observed in FTIR spectra of ACINA. The FTIR spectra of AC in ACINA shift in N-H stretching frequency from 3363 to 3280  $\text{cm}^{-1}$  and C-N stretching from 1216 to 1222  $\text{cm}^{-1}$ . Absorption peaks of C=O stretching of AC at 1650  $\text{cm}^{-1}$  did not shift but decreased in sharpness. The shifting of absorption peaks of AC in ACINA can correspond to hydrogen bond of the N-H and C-N group of AC with group of INA. The appearance of new FTIR spectra of ACINA is due to the occurrence of co-crystal formation via intermolecular interaction between AC and INA [20,21]. Overall, from the results of PXRD pattern DSC curve and FTIR spectra, the sample of ACINA may be concluded as a co-crystal.

Co-crystal physical properties are strongly influenced by the shape and size. SEM is a reliable method to analyze the morphology and particle size of the co-crystal [11,22]. The SEM analysis revealed that morphology of ACINA is different from the individual components.

AC has poorly water-soluble and highly permeable properties including a drug class II in biopharmaceutics classification system [3]. Modify of AC into ACINA co-crystal can significantly ( $p < 0.05$ ) increase the solubility of AC in distilled water. Co-crystal has the ability to increase solubility of drug possibly due to changing of crystal packing which reduces the lattice energy and/or increase the solvent affinity [9].

The dissolution test results indicate that ACINA co-crystal dissolves faster than the pure AC. The result has indicated that AC in ACINA co-crystal exhibited a dissolution rate 2-3 times faster than that of pure AC. The enhancement of dissolution rate of ACINA co-crystal can be explained by effects of changing crystal morphology of AC into ACINA co-crystal. The difference of ACINA co-crystal surface forms a new surface nature of the crystal. Thus, it changes the dissolution stage of the co-crystal. Overall, the increased dissolution rate of ACINA co-crystal appears as a combination of crystal packing and morphology changes in ACINA co-crystal [23].

## CONCLUSION

AC and INA in equimolar ratio are capable of forming a co-crystal by slow solvent evaporation method. ACINA co-crystal has a spherical shape with a rough surface. Modification of AC into ACINA co-crystal increases the solubility and dissolution rate of AC.

## DECLARATIONS

### Acknowledgement

The research was funded by DRPM of Ministry of Research and Technology of Higher Education of the Republic of Indonesia with DIPA number: 0.42.06-0/2016. We thank PT Dexa Medica for the provision of atorvastatin calcium used in this study.

### Conflict of Interest

No conflict of interest associated with this work.

### Contribution of Authors

The authors declare that this work was done by the authors named in this article and all liabilities pertaining to claims relating to the content of this article will be borne by them.

### Open Access

This is an Open Access article that uses a funding model which does not charge readers or their institutions for access and distributed under the terms of the Creative Commons Attribution License (<http://creativecommons.org/licenses/by/4.0>) and the Budapest Open Access Initiative (<http://www.budapestopenaccessinitiative.org/read>), which permit unrestricted use, distribution, and reproduction in any medium, provided the original work is properly credited.

## REFERENCES

1. Shete G, Puri V, Kumar L, Bansal AK. Solid state characterization of commercial crystalline and amorphous atorvastatin calcium samples. *Pharm Sci Tech* 2010; 11(2): 598-609.
2. Zhang HX, Wang JX, Zhang ZB, Le Y, Shen ZG, Chen JF. Micronization of atorvastatin calcium by antisolvent precipitation process. *Int J Pharm* 2009; 374: 106-113.
3. Anwar M, Warsi MH, Mallick N, Akhter S, Gahoi S, Jain GK, Talegaonkar S, Ahmad FJ, Khar RK. Enhanced bioavailability of nano-sized chitosan-atorvastatin conjugate after oral administration to rats. *Eur J Pharm Sci* 2011; 44: 241-249.

4. Choudhary A, Rana AC, Aggarwal G, Kumar V, Zakir F. Development and characterization of an atorvastatin solid dispersion formulation using skimmed milk for improved oral bioavailability. *Acta Pharm Sin B* 2012; 2(4): 421–428.
5. Shayanfar A, Ghavimi H, Hamishehkar H, Jouyban A. Coamorphous atorvastatin calcium to improve its physicochemical and pharmacokinetic properties. *J Pharm Pharm Sci* 2013; 16: 577-587.
6. Mashhadi SMA, Yunus U, Bhatti MH, Tahir MN. Isoniazid cocrystals with anti-oxidant hydroxy benzoic acids. *J Mol Struct* 2014; 1076: 446–452.
7. Wang JR, Yu X, Zhou C, Lin Y, Chen C, Pan G, Mei X. Improving the dissolution and bioavailability of 6-mercaptopurine via co-crystallization with isonicotinamide. *Bioorg Med Chem Lett* 2015; 25: 1036–1039.
8. Sowa M, Slepokura K, Matczak-Jon E. Solid-state characterization and solubility of a genistein–caffeine cocrystal. *Journal of Molecular Structure* 2014; 1076: 80–88.
9. Thakuria R, Deloria A, Jonesa W, Lipert MP, Roy L, Rodríguez-Hornedo N. Pharmaceutical cocrystals and poorly soluble drugs. *Int J Pharm* 2013; 453: 101-125.
10. Su H, He H, Tian Y, Zhao N, Sun F, Zhang X, Jiang Q, Zhu G. Syntheses and characterizations of two curcumin-based cocrystals. *Inorg Chem Commun* 2015; 55: 92–95.
11. Qiao N, Li M, Schlindwein W, Malek N, Davies A, Trappitt G. Pharmaceutical cocrystals: An overview. *Int J Pharm* 2011; 419: 1-11.
12. Maeno Y, Fukami T, Kawahata M, Yamaguchi K, Tagami T, Ozeki T, Suzuki T, Tomono K. Novel pharmaceutical cocrystal consisting of paracetamol and trimethylglycine, a new promising cocrystal former. *Int J Pharm* 2014; 473: 179–186.
13. Lin HL, Wu TK, Lin SY. Screening and characterization of cocrystal formation of metaxalone with short-chain dicarboxylic acids induced by solvent-assisted grinding approach. *Thermochim Acta* 2014; 575: 313– 321.
14. Niazi SK. *Handbook of Preformulation: Chemical, Biological, and Botanical Drugs*. New York: Informa Healthcare; 2007.
15. Chadha R, Kuhad A, Arora P, Kishor S. Characterisation and evaluation of pharmaceutical solvates of atorvastatin calcium by thermoanalytical and spectroscopic studies. *Chem Cent* 2012; 16: 114-129.
16. Hong C, Xie Y, Yao Y, Li G, Yuan X, Shen H. A Novel strategy for pharmaceutical cocrystal generation without knowledge of stoichiometric ratio: myricetin cocrystals and a ternary phase diagram. *Pharm Res* 2012; 32(1): 47-60.
17. Sharkar A, Rohani S. Cocrystals of acyclovir with promising physicochemical properties. *J Pharm Sci* 2015; 104: 98-105.
18. Patel JR, Carlton RA, Needham TE, Chichester CO, Vogt FG. Preparation, structural analysis, and properties of tenoxicam cocrystals. *Int J Pharm* 2012; 436: 685– 706.
19. Babu NJ, Sanphui P, Nangia A. Crystal engineering of stable temozolomide cocrystals. *Chem Asian J* 2012; 7: 2274-2285.
20. Zhang GC, Lin HL, Lin SY. Thermal analysis and FTIR spectral curve-fitting investigation of formation mechanism and stability of indomethacin-saccharin cocrystals via solid-state grinding process. *J Pharm Biomed Anal* 2012; 66: 162-169.
21. Hsu PC, Lin HL, Wang SL, Lin SY. Solid-state thermal behavior and stability studies of theophylline–citric acid cocrystals prepared by neat cogrinding or thermal treatment. *J Solid State Chem* 2012; 192: 238-245.
22. Padrela L, Rodrigues MA, Velaga SP, Matos HA, Azevedo EG. Formation of indomethacin–saccharin cocrystals using supercritical fluid technology. *Eur J Pharm Sci* 2009; 38: 9-17.
23. Blagden N, Matas M, Gavan PT, York P. Crystal engineering of active pharmaceutical ingredients to improve solubility and dissolution rates. *Adv Drug Deliv Rev* 2007; 59: 617-630.